

Overcoming the Curse of Dimensionality When Clustering Multivariate Volume Data

Vladimir Molchanov¹ and Lars Linsen^{1,2}

¹*Jacobs University, Bremen, Germany*

²*Westfälische Wilhelms-Universität Münster, Münster, Germany*

Keywords: Multi-dimensional Data Visualization, Multi-field Data, Clustering.

Abstract: Visual analytics of multidimensional data suffer from the curse of dimensionality, i.e., that even large numbers of data points will be scattered in a high-dimensional space. The curse of dimensionality prohibits the proper use of clustering algorithms in the high-dimensional space. Projecting the space before clustering imposes a loss of information and possible mixing of separated clusters. We present an approach where we overcome the curse of dimensionality for a particular type of multidimensional data, namely for attribute spaces of multivariate volume data. For multivariate volume data, it is possible to interpolate between the data points in the high-dimensional attribute space based on their spatial relationship in the volumetric domain (or physical space). We apply this idea to a histogram-based clustering algorithm. We create a uniform partition of the attribute space in multidimensional bins and compute a histogram indicating the number of data samples belonging to each bin. Only non-empty bins are stored for efficiency. Without interpolation, the analysis is highly sensitive to the cell sizes yielding inaccurate clustering for improper choices: Large cells result in no cluster separation, while clusters fall apart for small cells. Using tri-linear interpolation in physical space, we can refine the data by generating additional samples. The refinement scheme can adapt to the data point distribution in attribute space and the histogram's bin size. As a consequence, we can generate a density computation, where clusters stay connected even when using very small cell sizes. We exploit this result to create a robust hierarchical cluster tree. It can be visually explored using coordinated views to physical space visualizations and to parallel coordinates plots. We apply our technique to several datasets and compare the results against results without interpolation.

1 INTRODUCTION

Visualization of multivariate volume data has become a common, yet still challenging task in scientific visualization. Data sets come from traditional scientific visualization applications such as numerical simulations, see VisContest 2008 (Whalen and Norman, 2008), or medical imaging, see VisContest 2010 (Vis, 2010). While looking into individual attributes can be of high interest, the full phenomena are often only captured when looking into all attributes simultaneously. Consequently, visualization methods shall allow for the investigation and analysis of the multidimensional attribute space. The attribute space may consist of measured and/or simulated attributes as well as derived attributes including statistical properties (e.g., means, variances) or vector and tensor field properties (e.g., divergence, finite time Lyapunov exponent, diffusion tensor eigenvalues). Hence, we are facing a multidimensional data analysis task, where

dimension here refers to the dimensionality of the attribute space.

Multidimensional data analysis typically requires some automatic components that need to be used to produce a visual encoding. Typical components are clustering approaches or projections from higher-dimensional spaces into 2D or 3D visual spaces. Often, clustering and projections are combined to produce a visualization of a clustering result. The clustering approach shall be applied first to produce high-dimensional clusters, which can be used as an input for an improved projection. Unfortunately, clustering in a high-dimensional space faces the problem that points belonging to the same cluster can be rather far apart in the high-dimensional space. This observation is due to the curse of dimensionality, a term coined by Bellman (Bellman, 1957). It refers to the fact that there is an exponential increase of volume when adding additional dimensions.

The impact of the curse of dimensionality on prac-

tical issues when clustering high-dimensional data is as follows: Clustering approaches can be categorized as being based on distances between data points or being based on density estimates. However, only distance-based clustering algorithms can effectively detect clusters of arbitrary shape. Distance-based clustering approaches require local density estimates, which are typically based on space partitioning (e.g., over a regular or an adaptive grid) or on a kernel function. Both grid-based and kernel-based approaches require the choice of an appropriate size of locality for density estimation, namely, the grid cell size or the kernel size, respectively. Using a too large size leads to not properly resolving the clusters such that clusters may not be separated. Hence, a small size is required. However, due to the curse of dimensionality, clusters fall apart when using a too small size and one ends up with individual data points rather than clusters thereof.

Attribute spaces of multivariate volume data are a specific case of multidimensional data, as the unstructured data points in attribute space do have a structure when looking into the corresponding physical space. We propose to make use of this structure by applying interpolation between attribute-space data points whose corresponding representations in physical space exhibit a neighbor relationship.

The overall approach presented in this paper takes as input a multivariate volume data set. First, it applies an interpolation scheme to upsample the attribute space, see Section 4 for the main idea, Section 5 for an improved computation scheme, and Section 6 for an amendment to handle sharp material boundaries. The upsampled attribute space is, then, clustered using a hierarchical density-based clustering approach, see Section 3. Based on the clustering result, Section 7 describes how a combined visual exploration of physical and attribute space using coordinated views can be employed. The results of the approach are presented in Section 8 and its properties are discussed in Section 9. It is shown that our approach manages to produce high-quality clustering results without the necessity of tweaking the grid cell size or similar. We also document that comparable results cannot be obtained when clustering without the proposed interpolation step. The linked volume visualization, therefore, reflects the phenomena in the multivariate volume data more reliably.

2 RELATED WORK

2.1 Multivariate Volume Data Visualization

Traditionally, spatial data visualization focuses on one attribute, which may be scalar, vector, or tensor-valued. In the last decade, there was an increase on attempts to generalize the visualization methods to multivariate volume data that allow for the visual extraction of multivariate features. Sauber et al. (Sauber et al., 2006) suggested to use multigraphs to generate combinations of multiple scalar fields, where the number of nodes in the graph increase exponentially with the number of dimensions. Similarly, Woodring and Chen (Woodring and Shen, 2006) allowed for boolean set operations of scalar field visualization. In this context, Akiba and Ma (Akiba and Ma, 2007) and Blaas et al. (Blaas et al., 2007) were the first who used sophisticated visualization methods and interaction in the multi-dimensional attribute space. Akiba and Ma (Akiba and Ma, 2007) suggested a tri-space visualization that couples parallel coordinates in attribute space with volume rendering in physical space in addition to one-dimensional plots over time. Blaas et al. (Blaas et al., 2007) use scatter plots in attribute space, where the multi-dimensional data is projected into arbitrary planes. Daniels II et al. (Daniels II et al., 2010) presented an approach for interactive vector field exploration by brushing on a scatterplot of derived scalar properties of the vector field, i.e., a derived multivariate attribute space. However, their interactive attribute space exploration approach does not scale to higher-dimensional attribute spaces. Other approaches are based on statistics rather than interactive visual feature extraction: Jänicke et al. (Jänicke et al., 2007) use statistical measures to detect regions of a certain behavior in multi-dimensional volume data, while Oeltze et al. (Oeltze et al., 2007) use correlation and principal component analysis to visualize medical perfusion data.

Recently, there has been the approach to couple attribute space clustering with visual interactive exploration of multivariate volume data. Maciejewski et al. (Maciejewski et al., 2009) developed multi-dimensional transfer functions for direct volume rendering using 2D and 3D histograms and density-based clustering within these histograms. Since interactions with the histograms are necessary for visual analysis of the data, their approach is restricted to attribute spaces of, at most, three dimensions. Linsen et al. (Linsen et al., 2008; Linsen et al., 2009) proposed an approach that can operate on multivariate volume data with higher-dimensional attribute spaces. The at-

tribute space is clustered using a hierarchical density-based approach and linked to physical-space visualization based on surface extraction. Recently, the approach was extended by Dobrev et al. (Dobrev et al., 2011) to an interactive analysis tool incorporating direct volume rendering. Dobrev et al. show that the generated clustering result is often not as desired and propose interactive means to fix the clustering result. In this paper, we make use of the same clustering approach, see Section 3, and show how we can improve the results with the methods proposed here.

2.2 Clustering

Cluster analysis divides data into meaningful or useful groups (clusters). Clustering algorithms can be categorized with respect to their properties of being based on partitioning, hierarchical, based on density, or based on grids (Jain and Dubes, 1988; Han and Kamber, 2006). In partitioning methods, data sets are divided into k clusters and each object must belong to exactly one cluster. In hierarchical methods, data sets are represented using similarity trees and clusters are extracted from this hierarchical tree. In density-based methods, clusters are a dense region of points separated by low-density regions. In grid-based methods, the data space is divided into a finite number of cells that form a grid structure and all of the clustering operations are performed on the cells.

Hartigan (Hartigan, 1975; Hartigan, 1985) first proposed to identify clusters as high density clusters in data space. Wong and Lane (Wong and Lane, 1983) define neighbors for each data point in data space and use the k th nearest neighbors to estimate density. After defining dissimilarity between neighboring patterns, a hierarchical cluster tree is generated by applying a single-linkage algorithm. In their paper, they show that the high density clusters are strongly consistent. However, they do not examine modes of the density function.

Ester et al. (Ester et al., 1996) introduced the DBSCAN algorithm. The first step of the DBSCAN algorithm is to estimate the density using an Eps -neighborhood (like a spherical density estimate). Second, DBSCAN selects a threshold level set $MinPts$ and eliminates all points with density values less than $MinPts$. Third, a graph is constructed based on the two parameters Eps and $MinPts$. Finally, high density clusters are generated by connected components of the graph. The drawback is the need to define appropriate parameters. Hinneburg and Keim introduced the DENCLUE approach (Hinneburg and Keim, 1998), where high density clusters are identified by determining density attraction. Hinneburg et

al. further introduced the HD-Eye system (Hinneburg et al., 1999) that uses visualization to find the best contracting projection into a one- or two-dimensional space. The data are divided based on a sequence of the best projections determined by the high density clusters. The advantage of this method is that it does not divide regions of high density.

Ankerst et al. (Ankerst et al., 1999) introduced the OPTICS algorithm, which computes a complex hierarchical cluster structure and arranges it in a linear order that is visualized in the reachability plot. Stuetzle (Stuetzle, 2003) also used a nearest neighbor density estimate. A high density cluster is generated by cutting off all minimum spanning tree edges with length greater than a specific parameter (depending on the level-set value of the density function). Stuetzle and Nugent (Stuetzle and Nugent, 2007) proposed to construct a graph whose vertices are patterns and whose edges are weighted by the minimum value of the density estimates along the line segment connecting the two vertices. The disadvantage of this hierarchical density-based approach is that the hierarchical cluster tree depends on a threshold parameter (level-set value) that is difficult to determine.

We use a hierarchical density-based approach that computes densities over a grid. The main advantage of our approach is the direct identification of clusters without any threshold parameter of density level sets. Moreover, it is quite efficient and scales well. The main idea of the approach is described in Section 3. For a detailed analysis and comparison to other clustering approaches, which is beyond the scope of this paper, we refer to the literature (Long, 2009).

2.3 Interpolation in Attribute Space

Our main idea is based on interpolation in attribute space, which is possible due to a meaningful neighborhood structure in physical space that can be imposed onto the attribute space. Similar observations have been used in the concept of continuous scatterplots (Bachthaler and Weiskopf, 2008; Bachthaler and Weiskopf, 2009; Heinrich et al., 2011; Lehmann and Theisel, 2010; Lehmann and Theisel, 2011). Continuous scatterplots generalize the concept of scatterplots to the visualization of spatially continuous input data by a continuous and dense plot. The high-dimensional histograms we create can be regarded as a generalization of the 2D continuous histograms created by Bachthaler and Weiskopf (Bachthaler and Weiskopf, 2008). It is a more difficult problem to compute continuous histograms in high-dimensional spaces. However, in the end, we only need a discrete sampling of the continuous histogram.

Hence, our computations do not aim at computing continuous histograms, but rather stick to operating on a discrete setting.

3 CLUSTERING

We present a hierarchical density cluster construction based on nonparametric density estimation using multivariate histograms. Clusters can be identified without any threshold parameter of density level sets. Let the domain of the attribute space be given in form of a d -dimensional hypercube, i.e., a d -dimensional bounding box. To derive the density function, we spatially subdivide the domain of the data set into cells (or bins) of equal shape and size. Thus, the spatial subdivision is given in form of a d -dimensional regular structured grid with equidistant d -dimensional grid points, i.e., a d -dimensional histogram. For each bin of the histogram, we count the number of sample points lying inside. The multivariate density function is estimated by the formula

$$f(x) = \frac{n_{bin}}{n \cdot A_{bin}}$$

for any x within the cell, where n is the overall number of data points, n_{bin} is the number of data points inside the bin, and A_{bin} is the area of the d -dimensional bin. As the area A_{bin} is equal for all bins, the density of each bin is proportional to the number n_{bin} of data points lying inside the bin. Hence, it suffices to just operate with those numbers n_{bin} .

To estimate all non-empty bins, we use a partitioning algorithm that iterates through all dimensions. Figure 1 illustrates the partition process for a two-dimensional data set: The first dimension is divided into 5 equally-sized intervals on the left-hand side of Figure 1. Only four non-empty intervals are obtained. These intervals are subsequently divided in the second dimension, as shown on the right-hand side of Figure 1. The time complexity for partitioning the data space is $O(nd)$, i.e., it can handle both data sets with large number of samples n and data sets with high dimensionality d .

Given the d -dimensional histogram, clusters are defined as largest sets of neighboring non-empty bins, where neighboring refers to sharing a common vertex. To detect higher-density clusters within each cluster, we remove all cells containing the minimum number of points in this cluster and detect among the remaining cells, again, largest sets of neighboring cells. This step may lead to splitting of a cluster into multiple higher-density clusters. This process is iterated until no more clusters split. Recording the splitting information, we obtain a cluster hierarchy. Those clusters

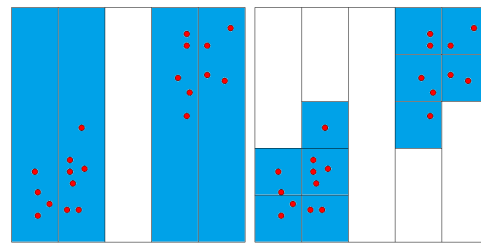


Figure 1: Grid partition of two-dimensional data set: The space is divided into equally-sized bins in the first dimension (left) and the non-empty bins are further subdivided in the second dimensions (right).

that do not split anymore represent local maxima and are referred to as mode clusters. Figure 2 (left) shows a set of non-empty cells with six different density levels in a two-dimensional space. First, we find the two low-density clusters as connected components of non-empty cells. They are represented in the cluster tree as immediate children nodes of the root node (cyan and yellow), see Figure 2 (right). From the cluster colored cyan, we remove all minimum density level cells (cyan). The cluster remains connected. Then, we again remove the cells with minimum density level (green). The cluster splits into three higher-density clusters (red, magenta, and blue). They appear as children nodes of the cyan node in the cluster tree. As densities are given in form of counts of data points, they are always natural numbers. Consequently, we cannot miss any split of a density cluster when iterating over the natural numbers (from zero to the maximum density). The time complexity to create a hierarchical density cluster tree is $O(m^2)$, where m is the number of non-empty cells.

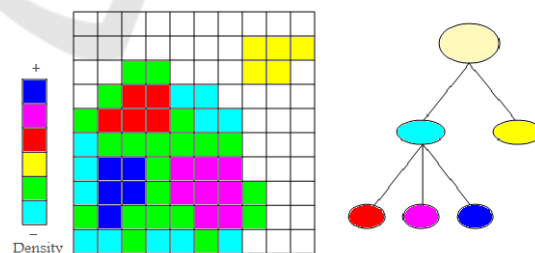


Figure 2: *Left:* Grid partition of two-dimensional data set with six different density levels. *Right:* Respective density cluster tree with four modes shown as leaves of the tree.

Figure 3 shows that the clustering approach is capable of handling clusters of any shape and that it is robust against changing cluster density and noise. Noise has been handled by removing all cells with a number of sample points smaller than a noise threshold. The data set is a synthetic one (Karypis et al., 1999). Figure 4 shows the visualization of a cluster

hierarchy for the “out5d” data set with 16,384 data points and five attributes, namely, spot (SPO), magnetics (MAG), potassium (POS), thorium (THO), and uranium (URA), using a projection in optimized 2D star coordinates (Long, 2009). The result seems feasible and all clusters were found without defining any density thresholds, but the choice of the bin size had to be determined empirically in an interactive visual analysis using coordinated views as described in this paper. Figure 5 shows how sensitive the result is to the bin size: Using smaller bin sizes merges some clusters, while using larger sizes makes clusters fall apart. The result in Figure 4 was obtained using the heuristic that cluster numbers only vary slowly close to the optimal bin size value (area marked red in Figure 4). However, in practice one would not generate results for the entire range of possible bin sizes for being able to apply this heuristic. Instead, one would rather use a trial-and-error approach, not knowing how reliable the result is.

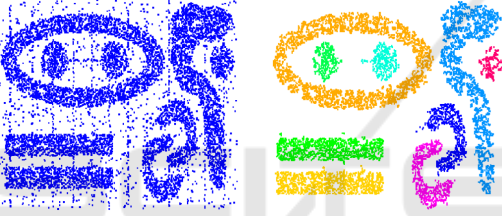


Figure 3: Clustering of arbitrarily shaped clusters. *Left:* Original data set. *Right:* Histogram-based clustering result.

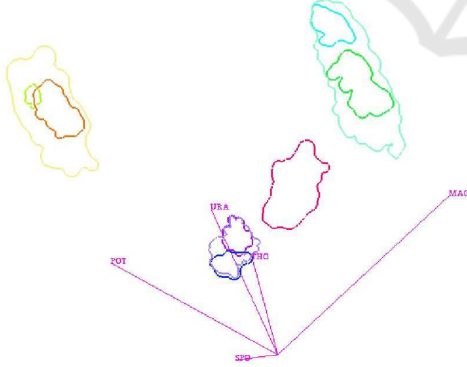


Figure 4: Visualization of cluster hierarchy in optimized 2D star coordinates.

4 INTERPOLATION

Let the attribute values of the multivariate volume data be given at points \mathbf{p}_i , $i = 1, \dots, n$, in physical space. Moreover, let $a_j(\mathbf{p}_i)$, $j = 1, \dots, d$, be the attribute values at \mathbf{p}_i . Then, the points \mathbf{p}_i exhibit some

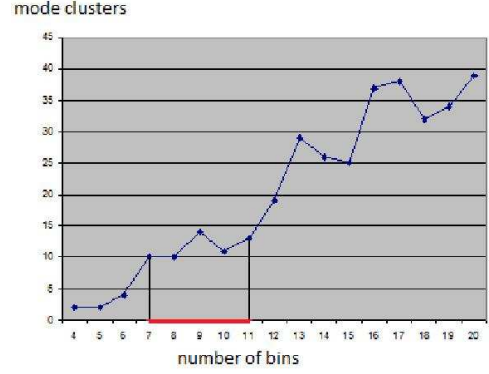


Figure 5: Sensitivity of clustering results with respect to the bin size. The graph plots the number of mode clusters over the number of bins per dimension.

neighborhood relationship in physical space. Typically, this neighborhood information is given in form of grid connectivity, but even if no connectivity is given, meaningful neighborhood information can be derived in physical space by looking at distances (e.g., nearest neighbors or natural neighbors). Based on this neighborhood information, we can perform an interpolation to reconstruct a continuous multivariate field over the volumetric domain. In the following, we assume that the points \mathbf{p}_i are given in structured form over a regular (i.e., rectangular) hexahedral grid. Thus, the reconstruction of a continuous multivariate field can be obtained by simple trilinear interpolation within each cuboid cell of the underlying grid. More precisely: Let \mathbf{q} be a point inside a grid cell with corner points \mathbf{p}_{uvw} , $u, v, w \in \{0, 1\}$, and let $(q_x, q_y, q_z) \in [0, 1]^3$ be the local Cartesian coordinates of \mathbf{q} within the cell. Then, we can compute the attribute values at \mathbf{q} by

$$a_j(\mathbf{q}) = \sum_{u=0}^1 \sum_{v=0}^1 \sum_{w=0}^1 q_x^u q_y^v q_z^w (1-q_x)^{1-u} (1-q_y)^{1-v} (1-q_z)^{1-w} a_j(\mathbf{p}_{uvw})$$

for all attributes ($j = 1, \dots, d$). In attribute space, we obtain the point $(a_1(\mathbf{q}), \dots, a_d(\mathbf{q}))$, which lies within the convex hull of the set of points $(a_1(\mathbf{p}_{uvw}), \dots, a_d(\mathbf{p}_{uvw}))$, $u, v, w \in \{0, 1\}$.

Now, we want to use the interpolation scheme to overcome the curse of dimensionality when creating the d -dimensional density histogram. Using the trilinear interpolation scheme, we reconstruct the multivariate field within each single cell, which corresponds to a reconstructed area in attribute space. The portion $r \in [0, 1]$ by which the reconstructed area in attribute space falls into a bin of the d -dimensional density histogram defines the amount of density that should be added to the respective bin of the histogram.

Under the assumption that each grid cell has volume $\frac{1}{c}$, where c is the overall number of grid cells, one should add the density $r \cdot \frac{1}{c}$ to the respective bin of the histogram. However, we propose to not compute r exactly for two reasons: First, the computation of the intersection of a transformed cuboid with a d -dimensional cell in a d -dimensional space can be rather cumbersome and expensive. Second, the resulting densities that are stored in the bins of the histogram would no longer be natural numbers. The second property would require us to choose density thresholds for the hierarchy generation. How to do this without missing cluster splits is an open question.

Our approach is to approximate the reconstructed multivariate field by upsampling the given data set. This discrete approach is reasonable, as the output of the reconstruction/upsampling is, again, a discrete structure, namely a histogram. We just need to assure that the rate for upsampling is high enough such that the histogram of an individual grid cell has all non-empty bins connected. Thus, the upsampling rate depends on the size of the histogram's bins. Moreover, if we use the same upsampling rate for all grid cells, density can still be measured in form of number of (upsampled) data points per bin. Hence, the generation of the density-based cluster hierarchy is still working as before.

Figure 6 shows the impact of upsampling in the case of a 2D physical space and a 2D attribute space, i.e., for a transformed 2D cell with corners $\mathbf{a}_{uv} = (a_1(\mathbf{p}_{uv}), \dots, a_d(\mathbf{p}_{uv}))$, $u, v \in \{0, 1\}$, and a histogram with $d = 2$ dimensions. Without the upsampling, the non-empty bins of the histogram are not connected. After upsampling, the bins between the original non-empty bins have also been filled and the 2D cell represents a continuous region in the 2D attribute space.

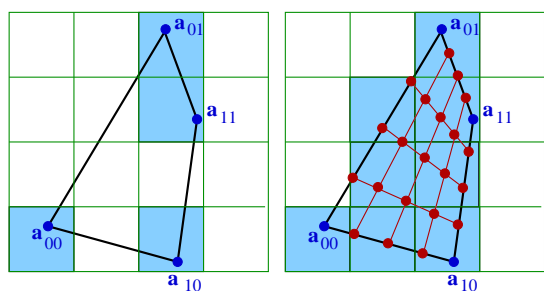


Figure 6: Upsampling for a 2D physical space and a 2D attribute space. *Left:* The corner points of the 2D cell correspond to bins of the histogram that are not connected. *Right:* After upsampling, the filled bins of the histogram are connected.

When performing the upsampling for all cells of the volumetric grid, we end up with a histogram, where all non-empty cells are connected. Hence, we

have overcome the curse of dimensionality. On such a histogram, we can generate the density-based cluster hierarchy without the effect of clusters falling apart.

5 ADAPTIVE SCHEME

In order to assure connectivity of non-empty histogram bins, we have to upsample in some regions more than in other regions. As we want to have a global upsampling rate, some regions may be oversampled. Such an oversampling is not a problem in terms of correctness, but a waste of computation time. To reduce computation time, we propose to use an adaptive scheme for upsampling. Since we are dealing with cuboid grid cells, we can adopt an octree scheme: Starting with an original grid cell, we upsample with a factor of two in each dimension. The original grid cell is partitioned into eight subcells of equal size. If the corners of a subcell S all correspond to one and the same histogram bin B , i.e., if $(a_1(\mathbf{p}_{uvw}), \dots, a_d(\mathbf{p}_{uvw}))$ fall into the same bin B for all corners \mathbf{p}_{uvw} , then we can stop the partitioning S . If the depth of the octree is d_{\max} and we stop partitioning S at depth d_{stop} , we increase the bin count (or density, respectively) of bin B by $8^{d_{\max} - d_{\text{stop}}}$. If the corners of a subcell S do not correspond to the same histogram bin, we continue with the octree splitting of S until we reach the maximum octree depth d_{\max} .

Memory consumption is another aspect that we need to take into account, since multivariate volume data per se are already quite big and we further increase the data volume by applying an upsampling. However, we can march through each original cell, perform the upsampling for that cell individually, and immediately add data point counts to the histogram. Hence, we never need to store the upsampled version of the full data. However, we need to store the histogram, which can also be substantial as bin sizes are supposed to be small. We handle the histogram by storing only non-empty bins in a dynamic data structure.

6 SHARP MATERIAL BOUNDARIES

Some data like the ones stemming from medical imaging techniques may exhibit sharp material boundaries. It is inappropriate to interpolate across those boundaries. In practice, such abrupt changes in attribute values may require our algorithm to execute many interpolation steps. To avoid interpolation

across sharp feature boundaries, we introduce a user-specified parameter that defines sharp boundaries. As this is directly related to the number of interpolation steps, the user just decides on the respective maximal number of interpolation steps d_{\max} . If two neighboring points in physical space have attribute values that lie in histogram cells that would not get connected after d_{\max} interpolation steps, we do not perform any interpolation between those points. This is important, as performing some few interpolation steps across sharp material boundary may introduce noise artifacts leading to artificial new clusters.

7 INTERACTIVE VISUAL EXPLORATION

After having produced a clustering result of the attribute space that does not suffer from the curse of dimensionality, it is, of course, of interest to also investigate the clusters visually in physical and attribute space. Hence, we want to visualize, which regions in physical space belong to which attribute space cluster and what are the values of the respective attributes.

For visualizing the attribute space clusters we make use of the cluster tree, see Figure 2 (right), and visualize it in a radial layout, see Figure 8 (lower row). The cluster tree functions as an interaction widget to select any cluster or any set of clusters. The properties of the selected clusters can be analyzed using a linked parallel coordinates plot that shows the function values in attribute space, see Figure 10 (middle row).

The distribution of the selected clusters in volume space can be shown in a respective visualization of the physical space. We support both a direct volume rendering approach and a surface rendering approach. The 3D texture-based direct volume renderer takes as input only the density values stemming from the clustering step and the cluster indices, see (Dobrev et al., 2011). Similarly, we extract boundary surfaces of the clusters using a standard isosurface extraction method, see Figure 10 (bottom). We illuminate our renderings using normals that have been derived as gradients from the density field that stems from the clustering approach.

8 RESULTS

First, we demonstrate on a simple scalar field example how our approach works and show that the discrete histogram of interpolated data approaches the contin-

uous analogon as the interpolation depth increases. Let scalar field $f(r)$ be defined as follows:

$$f(r) = \begin{cases} br^2 & \text{for } r \geq 0.8, \\ 1 & \text{else,} \end{cases} \quad b = 0.85/0.8^2,$$

where r stands for the Euclidean distance to the center of domain $[-1, 1]^3$, see Figure 7 (left). The continuous histogram $h(x)$ can be computed using the relation

$$\int_0^r h(x) dx = \frac{4\pi}{3} [f^{-1}(r)]^3, \quad 0 \leq r \leq 0.8,$$

which leads to

$$h(r) = \frac{4\pi}{a^{3/2}} \sqrt{r}, \quad 0 \leq r \leq 0.8.$$

The continuous histogram is plotted in Figure 7 (right). The continuous data are clearly separated into two clusters, which represent the interior of a sphere and the background in physical space. However, when sampling the field at 30³ regular samples in the physical domain. the use of 100 bins in the attribute space leads to the effect that the sphere cluster breaks into many small parts. In Figure 8, we demonstrate how our interpolation approach corrects the histogram (upper row) and the respective cluster tree (lower row). The resulting discrete histograms approach the shape of the continuous one as upsampling depth grows. Depth $d_{\max} = 7$ is needed to converge to the correct result of the two clusters.

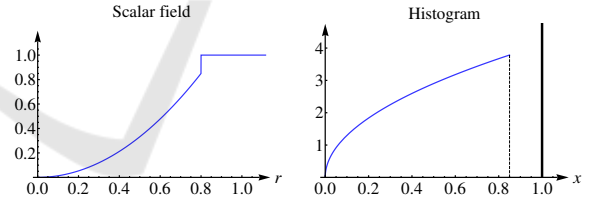


Figure 7: Scalar field distribution (left) and continuous histogram (right) for artificial data. Bold vertical line denotes the scaled Dirac function in the histogram.

Second, we design a volumetric multi-attribute data set, for which the ground truth is known, show how the size of bins affects the result of the clustering procedure and demonstrate that interpolation helps to resolve the issue. Given physical domain $[-1; 1]^3$, we use the following algebraic surfaces

$$F_1(x, y, z) = x^2 - y^2 - 5z = 0, \quad (1)$$

$$F_2(x, y, z) = x^2 + y^2 + (z - 1)z^2 = 0, \quad (2)$$

see Figure 9 (left). We construct the distributions of two attributes as functions of algebraic distances to the surfaces above, i.e.,

$$f_i = f_i(F_i(x, y, z)), \quad i = 1, \dots, 2.$$

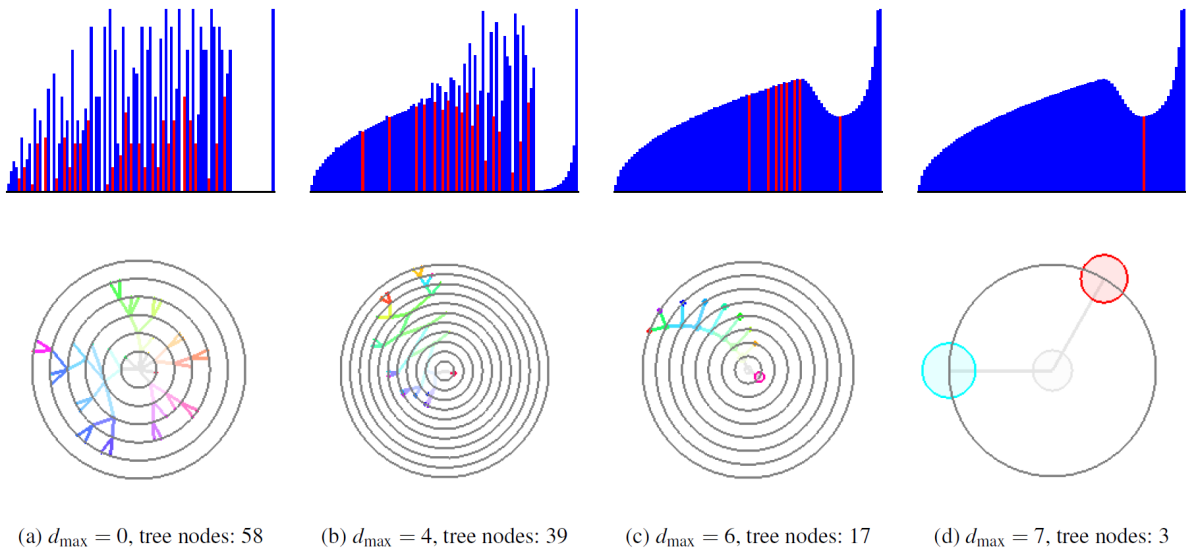


Figure 8: Discrete histograms with 100 bins each and cluster trees at different interpolation depth for data in Figure 7. Red bins are local minima corresponding to branching in trees. Interpolation makes histograms approach the form of continuous distribution and corrects cluster tree.

Functions f_i are chosen to have a discontinuity or a large derivative at the origin, respectively, see Figure 9 (middle). Thus, the surfaces F_i are cluster boundaries in the physical space. The distribution of the attribute values f_i is shown in a 2D scatterplot in Figure 9 (right) when sampling over a regular grid with 50^3 nodes. The data represent four clusters. Using 10 bins for each attribute to generate the histogram is not enough to separate all clusters resulting in a cluster tree with only 2 clusters as shown in Figure 10 (upper row). A larger number of bins is necessary. When increasing the number of bins to 30 for each attribute clusters fall apart due to the curse of dimensionality, which leads to a noisy result with too many clusters, see Figure 10 (middle row). However, applying four interpolation steps fixes the histogram. Then, the cluster tree has the desired four leaves and the boundary for all four clusters are correctly detected in physical space, see Figure 10 (lower row).

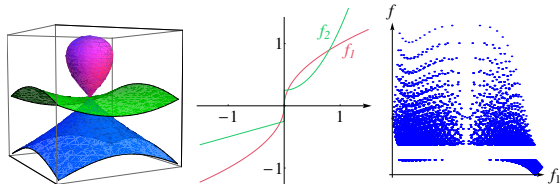


Figure 9: Designing a synthetic dataset: Algebraic surfaces separate clusters in physical space (left). Functions of algebraic distance to the surfaces (middle) define distribution of two attributes. The resulting distribution in the attribute space in form of a 2D scatterplot (right).

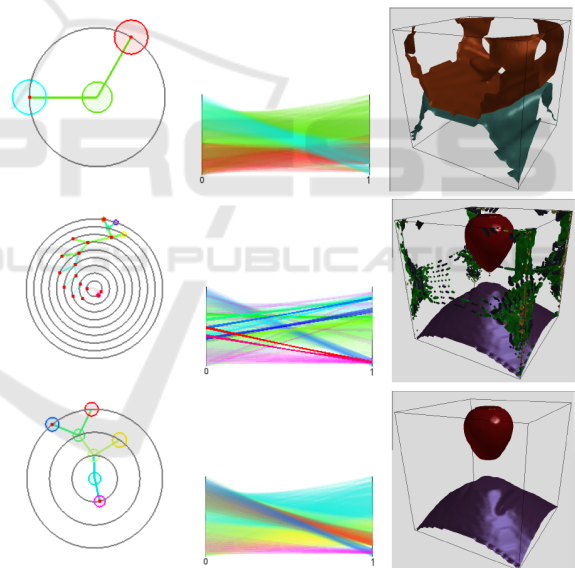


Figure 10: Effect of bin size choice and interpolation procedure on synthetic data with known ground truth. 10^2 bins are not enough to separate all clusters resulting in a degenerate tree (upper row). 30^2 bins are too many to keep clusters together (middle row). Interpolation of data with the same number of bins corrects the tree (lower row). Cluster trees, parallel coordinates, and clusters in physical space are shown in the left, mid, and right columns, correspondingly. Matching colors are used in the coordinated views to allow for analyzing correspondences.

Next, we apply our methods to the simulation-based dataset provided in the 2008 IEEE Visualization Design Contest (Whalen and Norman, 2008) and quantify the gain of (modified) adaptive upsampling.

We picked time slice 75 of this ionization front instability simulation. We considered the 10 scalar fields (mass density, temperature, and mass fractions of various chemical elements). What is of interest in this dataset are the different regions of the transition phases between atoms and ions of hydrogen (H) and helium (He). To reduce computational efforts, we made use of the symmetry of the data with respect to the $y = 124$ and the $z = 124$ planes and restricted consideration to data between $x = 275$ and $x = 500$ localizing the front. When applying the clustering approach to the original attribute space using a 10-dimensional histogram with 10 bins in each dimension, we obtain a cluster tree with 15 mode clusters. The cluster tree and the corresponding parallel coordinates plot are shown in Figure 11(a). Not all of the clusters are meaningful and some of them should have been merged to a single cluster. These mode clusters are not clearly separated when observing the parallel coordinates plot. After applying our approach with $d_{\max} = 5$, such clusters were merged leading to 12 modes and a simplified cluster tree. Results are shown in Figure 11(b). The timings of adaptive and non-adaptive upsampling for different interpolation depths are given in Table 1. “Modified adaptive” upsampling refers to the approach with no upsampling across sharp material boundaries, see Section sec:sharp. The adaptive schemes lead to a significant speed up (up to one order of magnitude). All numerical tests presented in this section were performed on a PC with an Intel Xeon 3.20GHz processor.

Table 1: Computation times for non-adaptive vs. adaptive upsampling scheme at different upsampling depths (2008 IEEE Visualization Design Contest dataset).

d_{\max}	0	1	2	3	4
Non-adaptive	7.57s	59.84s	488.18s	3929s	27360s
Adaptive	5.99s	27.5s	136.56s	717.04s	3646s
Non-empty bins	1984	3949	6400	9411	12861
Modified adaptive	14.3s	26.0s	80.91s	437.76s	2737s
Non-empty bins	1984	2075	2451	3635	5945

Finally, we demonstrate that scatterplots of upsampled data approach the quality of continuous scatterplots as presented by Bachthaler and Weiskopf (Bachthaler and Weiskopf, 2008) and the follow-up papers. The “tornado” dataset was sampled on a uniform grid of resolution 128^3 . Similar to (Bachthaler and Weiskopf, 2008), the magnitude of the velocity and the velocity in z -direction were taken as two data dimensions. In Figure 12, we show scatterplots of the original data and of the adaptively upsampled data with interpolation depth 5. The number of bins is 300 for each attribute. The quality of the upsampled scatterplot is similar to the continuous scatterplot presented in (Bachthaler and Weiskopf, 2008). We would like to note that rigorously speaking, eval-

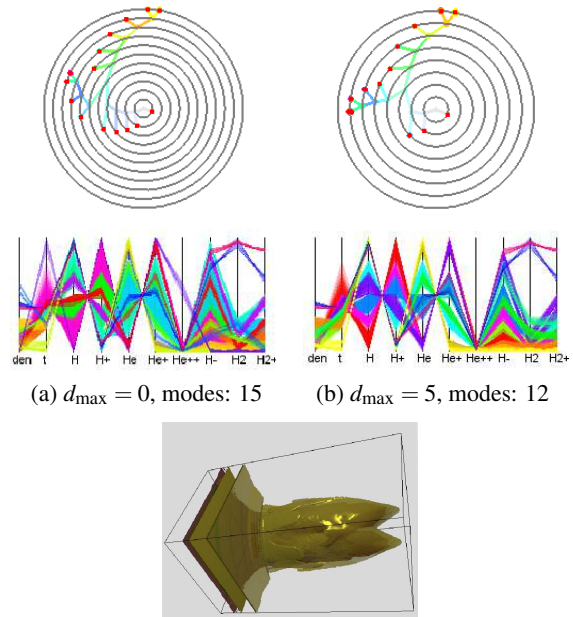


Figure 11: Cluster tree (upper row), parallel coordinates plot (middle row), and physical space visualization (lower row) for the 2008 IEEE Visualization Design Contest data set, time slice 75, for original attribute space using a 10-dimensional histogram (a) before and (b) after interpolation. Several mode clusters are merged when applying our approach, which leads to a simplification of the tree and better cluster separation. Matching colors are used in the coordinated views to allow for analyzing correspondences.

uation of vector magnitude and interpolation are not commutative operations. Thus, the upsampling with respect to the first chosen parameter could have significant errors in both the continuous and the discrete setting. However, we intentionally followed this way to be able to compare our results with results presented in (Bachthaler and Weiskopf, 2008).

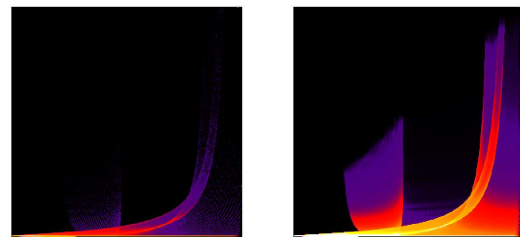


Figure 12: Scatterplots of the “tornado” dataset initially sampled on 128^3 regular grid. Original data (left) and result of adaptive upsampling with interpolation depth 5 (right) are shown.

9 DISCUSSION

Histogram Bin Size. The size of the bins of the histogram can be chosen arbitrarily. Of course, smaller bin sizes produce better results, as they can resolve better the shape of the clusters. Too large bin sizes lead to an improper merging of clusters. In terms of clustering quality, bin sizes can be chosen arbitrarily small, as very small bin sizes do not affect the clustering result negatively. However, storing a high-dimensional histogram with small bin sizes can become an issue. Our current implementation stores the histogram in main memory, which limits the bin sizes we can currently handle. This in-core solution allows us to produce decent results, as we are only storing non-empty bins. Nevertheless, for future work, it may still be desirable to implement an out-of-core version of the histogram generation. This can be achieved by splitting the histogram into parts and only storing those parts. However, an out-of-core solution would negatively affect the computation times. Also, the smaller the bin sizes, the more upsampling is necessary.

Upsampling Rate. The upsampling rate is influenced by the local variation in the values of the multivariate field and the bin size of the histogram. Let s_{bin} be the bin size of the histogram. Then, an upsampling may be necessary, if two data points in attribute space are more than distance s_{bin} apart. As the upsampling rate is defined globally, it is determined by the largest variation within a grid cell. Let s_{data} is the maximum distance in attribute space between two data points, whose corresponding points in physical space belong to one grid cell. Then, the upsampling rate shall be larger than $\frac{s_{data}}{s_{bin}}$. This ratio refers to the upsampling rate per physical dimension.

When using the adaptive scheme presented in Section 5, the upsampling rate per dimension is always a power of two. When a sufficiently high upsampling rate has been chosen, the additional computations when upsampling with the next-higher power of two in the adaptive scheme are modest, as computations for most branches of the octree have already terminated.

10 CONCLUSION

We presented an approach for multivariate volume data visualization that is based on clustering the multi-dimensional attribute space. We overcome the curse of dimensionality by upsampling the attribute space according to the neighborhood relationship in

physical space. Trilinear interpolation is applied to the attribute vectors to generate multidimensional histograms, where the support, i.e., all non-empty bins, is a connected component. Consequently, the histogram-based clustering does not suffer from clusters falling apart when using small bin sizes. We apply a hierarchical clustering method that generates a cluster tree without having to pick density thresholds manually or heuristically. In addition to a cluster tree rendering, the clustering results are visualized using coordinated views to parallel coordinates for an attribute space rendering and to physical space rendering. The coordinated views allows for a comprehensive analysis of the clustering result.

ACKNOWLEDGMENTS

This work was supported by the Deutsche Forschungsgemeinschaft (DFG) under project grant LI 1530/6-2.

REFERENCES

- (2010). Competition data set and description. 2010 IEEE Visualization Design Contest, <http://viscontest.sdsc.edu/2010/>.
- Akiba, H. and Ma, K.-L. (2007). A tri-space visualization interface for analyzing time-varying multivariate volume data. In *In Proceedings of Eurographics/IEEE VGTC Symposium on Visualization*, pages 115–122.
- Ankerst, M., Breunig, M. M., Kriegel, H.-P., and Sander, J. (1999). Optics: ordering points to identify the clustering structure. In *Proceedings of the 1999 ACM SIGMOD international conference on Management of data*, pages 49 – 60.
- Bachthaler, S. and Weiskopf, D. (2008). Continuous scatterplots. *IEEE Transactions on Visualization and Computer Graphics (Proceedings Visualization / Information Visualization 2008)*, 14(6):1428–1435.
- Bachthaler, S. and Weiskopf, D. (2009). Efficient and adaptive rendering of 2-d continuous scatterplots. *Computer Graphics Forum (Proc. Eurovis 09)*, 28(3):743 – 750.
- Bellman, R. E. (1957). *Dynamic programming*. Princeton University Press.
- Blaas, J., Botha, C. P., and Post, F. H. (2007). Interactive visualization of multi-field medical data using linked physical and feature-space views. In *EuroVis*, pages 123–130.
- Daniels II, J., Anderson, E. W., Nonato, L. G., and Silva, C. T. (2010). Interactive vector field feature identification. *IEEE Transactions on Visualization and Computer Graphics*, 16:1560–1568.

- Dobrev, P., Long, T. V., and Linsen, L. (2011). A cluster hierarchy-based volume rendering approach for interactive visual exploration of multi-variate volume data. In *Proceedings of 16th International Workshop on Vision, Modeling and Visualization (VMV 2011)*, pages 137–144. Eurographics Association.
- Ester, M., Kriegel, H.-P., Sander, J., and Xu, X. (1996). A density-based algorithm for discovering clusters in large spatial databases with noise. In *Proceedings of the second international conference on knowledge discovery and data mining*, page 226231.
- Han, J. and Kamber, M. (2006). *Data Mining: Concepts and Techniques*. Morgan Kaufmann Publishers.
- Hartigan, J. A. (1975). *Clustering Algorithms*. Wiley.
- Hartigan, J. A. (1985). Statistical theory in clustering. *Journal of Classification*, 2:62–76.
- Heinrich, J., Bachthaler, S., and Weiskopf, D. (2011). Progressive splatting of continuous scatterplots and parallel coordinates. *Comput. Graph. Forum*, 30(3):653–662.
- Hinneburg, A. and Keim, D. (1998). An efficient approach to clustering in large multimedia databases with noise. In *Proceedings of the fourth international conference on knowledge discovery and data mining*, page 5865.
- Hinneburg, A., Keim, D. A., and Wawryniuk, M. (1999). Hd-eye: Visual mining of high-dimensional data. *IEEE Computer Graphics and Applications*, pages 22–31.
- Jain, A. K. and Dubes, R. C. (1988). *Algorithms for Clustering Data*. Prentice Hall.
- Jänicke, H., Wiebel, A., Scheuermann, G., and Kollmann, W. (2007). Multifield visualization using local statistical complexity. *IEEE Transaction on Visualization and Computer Graphics*, 13(6):1384–1391.
- Karypis, G., Han, E. H., and Kumar, V. (1999). Chameleon: Hierarchical clustering using dynamic modeling. *Computer*, 32(8):68–75.
- Lehmann, D. J. and Theisel, H. (2010). Discontinuities in continuous scatter plots. *IEEE Transactions on Visualization and Computer Graphics*, 16:1291–1300.
- Lehmann, D. J. and Theisel, H. (2011). Features in continuous parallel coordinates. *Visualization and Computer Graphics, IEEE Transactions on*, 17(12):1912–1921.
- Linsen, L., Long, T. V., and Rosenthal, P. (2009). Linking multi-dimensional feature space cluster visualization to surface extraction from multi-field volume data. *IEEE Computer Graphics and Applications*, 29(3):85–89. linsenlongrosenthalvcgl.
- Linsen, L., Long, T. V., Rosenthal, P., and Rosswog, S. (2008). Surface extraction from multi-field particle volume data using multi-dimensional cluster visualization. *IEEE Transactions on Visualization and Computer Graphics*, 14(6):1483–1490. linsenlongrosenthalrosswogvcglsmoothvis.
- Long, T. V. (2009). *Visualizing High-density Clusters in Multidimensional Data*. PhD thesis, School of Engineering and Science, Jacobs University, Bremen, Germany.
- Maciejewski, R., Woo, I., Chen, W., and Ebert, D. (2009). Structuring feature space: A non-parametric method for volumetric transfer function generation. *IEEE Transactions on Visualization and Computer Graphics*, 15:1473–1480.
- Oeltze, S., Doleisch, H., Hauser, H., Muigg, P., and Preim, B. (2007). Interactive visual analysis of perfusion data. *IEEE Transaction on Visualization and Computer Graphics*, 13(6):1392–1399.
- Sauber, N., Theisel, H., and Seidel, H.-P. (2006). Multifield-graphs: An approach to visualizing correlations in multifield scalar data. *IEEE Transactions on Visualization and Computer Graphics*, 12(5):917–924.
- Stuetzle, W. (2003). Estimating the cluster tree of a density by analyzing the minimal spanning tree of a sample. *Journal of Classification*, 20:25–47.
- Stuetzle, W. and Nugent, R. (2007). A generalized single linkage method for estimating the cluster tree of a density. *Technical Report*.
- Whalen, D. and Norman, M. L. (2008). Competition data set and description. 2008 IEEE Visualization Design Contest, <http://vis.computer.org/VisWeek2008/vis/contests.html>.
- Wong, A. and Lane, T. (1983). A kth nearest neighbor clustering procedure. *Journal of the Royal Statistical Society, Series B*, 45:362–368.
- Woodring, J. and Shen, H.-W. (2006). Multi-variate, time varying, and comparative visualization with contextual cues. *IEEE Transactions on Visualization and Computer Graphics*, 12(5):909–916.